

## Histological and Morphometric Study on the Effect of Triiodothyronine on the Histological Changes of Gastrocnemius Muscle of Aged Male Albino Rat Associated with Thyroid Dysfunction

Asmaa Ibrahim Ahmed<sup>1</sup>, Sahar M. El Agaty<sup>2</sup> and Sayed M El- Sayed<sup>1</sup>

<sup>1</sup>Department of Anatomy and Embryology, <sup>2</sup>Department of Physiology, Faculty of Medicine, Ain Shams University, Cairo, Egypt

### ABSTRACT

**Introduction:** Aging associated with thyroid dysfunction induces many microstructural changes in the skeletal muscle fibers. These were caused by low T3, hyperglycemia and hyperinsulinemia. Triiodothyronine (T3) supplementation alleviates hyperglycemia and ameliorates insulin insensitivity of senile skeletal muscles.

**Aim of the Work:** Was to evaluate the histological changes of the senile albino rat gastrocnemius muscle associated with thyroid dysfunction as well as biochemical variations and the possible protective role of Triiodothyronine (T3).

**Material and Methods:** Thirty male albino rats were used. The rats were divided into three groups, with ten rats in each group. Adult group I; senile group II and T3 treated senile rats group III. T3 was administered at a dose of 8 µg/kg body weight for 2 weeks. At the end of the experiment, gastrocnemius muscles were dissected out and prepared for Hx&E stain, Masson's trichrome stain, Toluidine blue stained semi -thin sections and ultra-thin sections for electron microscopic study and morphometric measures were done.

**Results:** Skeletal muscle of senile group II showed thinning out and pyknosis of nuclei of muscle fibers. Ultrathin sections of senile rats showed abnormally-shaped degenerated mitochondria. Statistically significant decrease in thickness of muscle fibers and increase in collagen fiber deposition in group II. Group III showed restoration of the normal architecture of skeletal muscle fibers. The statistically significant increase in fasting glucose and insulin that was detected in group II was controlled in group III.

**Conclusion:** Aging associated with thyroid dysfunction in albino rats revealed marked structural changes in skeletal muscle and these changes were controlled by T3 supplementation through its ability to increase insulin sensitivity. This can be considered clinically to perform further studies for using T3 in geriatrics suffering from sarcopenia associated with thyroid dysfunction.

**Received:** 17 September 2022, **Accepted:** 08 November 2022

**Key Words:** Aging, electron microscopy, gastrocnemius muscle, morphometry, triiodothyronine (T3).

**Corresponding Author:** Asmaa Ibrahim Ahmed, PhD, Department of Anatomy and Embryology, Faculty of Medicine, Ain Shams University, Cairo, Egypt, **Tel.:** +20 10 0766 7294, **E-mail:** asmaaibrahim96@yahoo.com

**ISSN:** 1110-0559, Vol. 47, No. 1

### INTRODUCTION

Senility or aging is markedly accompanied by difficult glucose utilization by the tissues which is termed glucose intolerance and consequently disturbed glucose homeostasis ensues as in diabetes mellitus (type 2)<sup>[1]</sup>. Disruption of glucose metabolism occurs commonly with defective insulin sensitivity that is linked with diminished glucose uptake by different tissues<sup>[2]</sup>. Insulin has vital contribution in the skeletal muscle consumption of glucose. The microstructural alterations in the striated muscles in geriatrics participate in the occurrence of insulin resistance (IR) demonstrated in advancing age<sup>[3]</sup>. Mohamed *et al.*<sup>[4]</sup> demonstrated a reduction in the essential carrier proteins for utilization of glucose by most of the striated or skeletal limb muscles specially in advancing age. Prompt treatment of IR in elderly is vital for ameliorating and preventing hazards of hyperglycemia.

Thyroid hormones activate the glucose metabolism<sup>[5]</sup>. They act through stimulation of certain carrier proteins and enzymes<sup>[6]</sup>. Disturbed thyroid functions whether augmentation or reduction have been accompanied by interruption of glucose metabolism and insulin signaling in some elders<sup>[7]</sup>. Many studies concluded that elevated thyroid stimulating hormone (TSH) and reduced free thyroxine (fT4) are connected to IR<sup>[8]</sup>. Furthermore, researchers tested thyroid hormone provision in IR cases and reached favorable outcomes<sup>[3]</sup>. Prieto-Almeida *et al.*<sup>[9]</sup> stated that triiodothyronine (T3) supplementation could alleviate hyperglycemia and ameliorate IR of striated muscle and many other tissues in diabetic rats and similarly in obese rats.

Thus, the current work aimed to investigate the possible structural aberrations and histological changes that could be encountered in gastrocnemius muscle of senile rats and

if the thyroid hormone supplementation could improve these changes by improvement of glucose and insulin levels using light and electron microscopy in addition to morphometry.

## MATERIALS AND METHODS

### Animals

Thirty male albino rats were obtained. Ten young adult (3 – 4-month-old, body weight  $190 \pm 10$  g) and 20 aged (20 – 24-month-old, body weight  $405.2 \pm 22.4$  g). Rats were gained from Helwan Farm, Cairo, Egypt. They were kept under constant 12 h/12 h day/night period in the Medical Ain Shams Research institute (MASRI), Faculty of Medicine, Ain Shams University. Rats were nourished normal rat chow and allowed free approach to food and water ad libitum. All experimental steps were accomplished according to the instructions of FMASU, REC (Faculty of Medicine, Ain Shams University, Research Ethics Committee, Cairo, Egypt) that comply with the Guide for the Care and Use of Laboratory Animals released by United States National Institute of Health.

### Experimental design

Rats were divided randomly into three groups: 1) adult group (I) (n = 10; rats given intraperitoneal (i.p.) injection of the hormone vehicle); 2) **aged group (II)** (n = 10; rats received i.p. of the hormone vehicle), and 3) **T3-aged group (III)** (n = 10; triiodo-thyronine-treated aged group – rats given 3,3',5-triiodo-L-thyronine) (Sigma, St. Louis, MO, USA) that was in 1 N of NaOH/isotonic saline dissolve and given i.p. at a dose of 8 µg/ kg body weight per day for 2 weeks<sup>[10]</sup>. On the 15th day, at 9 a.m. the rats were weighed and received intraperitoneal injection of sodium thiopental (40 mg/kg). A midline abdominal cut was done, the abdominal aorta was bare, a polyethylene catheter was inserted into it, and a blood sample was assembled in a plastic tube. At room temperature, blood was permitted to clot, centrifuged at 3000 rpm for 15 min and serum was stored at -20°C, till applied for assessment of serum levels of free triiodothyronine (FT3), fasting glucose and insulin levels.

### Biochemical analysis

Measurement of fasting serum glucose was done by oxidase-peroxidase method<sup>[11]</sup>. Serum levels of insulin and FT3 were tested by enzyme-linked immunosorbent assay ELISA (Dako, Carpinteria, CA, and Cusabio, USA, respectively) according to the manufacturer's directions.

### Sample collection

At the end of the experimental stage (after 2 weeks), all rats received anesthesia. After taking blood samples for biochemical assays, the gastrocnemius muscles were carefully dissected, obtained, and cut longitudinally to be subjected to different histological preparations. Specimens were processed for paraffin, semithin and ultrathin sections to be examined by the light and electron microscopy.

### For light microscopic studies

At the end of the experiment the animals were sacrificed. Gastrocnemius muscles were dissected out. The specimens were prepared for the following:

1. Hematoxylin and Eosin (H&E) staining technique.
2. Masson's trichrome (MTC) stain to detect the collagenous fibers distribution and muscle fibrosis<sup>[12]</sup>.

All Sections were investigated and photographed with Olympus BX 40 light microscope (Olympus, Hamburg, Germany) linked to a camera Canon power shot A640 digital camera (Canon Inc., Tokyo, Japan) at Anatomy Department, Faculty of Medicine, Ain Shams University.

### For electron microscopic studies

Animals were injected by glutaraldehyde intracardiac for good E.M. results. Small pieces 1 mm<sup>3</sup> in size were taken from Gastrocnemius muscle. The specimens were fixed in 3% phosphate buffered glutaraldehyde (PH 7.3). Then the specimens were post fixed in 1% osmium tetroxide. Dehydration was done in ascending grades of alcohol. The specimens were cleared in propylene oxide at room temperature. The specimens were infiltrated by epon gradually till tissues kept in pure epon. Specimens were mounted in gelatin capsules filled with fresh epon. The capsules were kept in oven at 60° C to allow polymerization. Semithin sections were cut and stained by toluidine blue. Ultrathin sections were cut on ultramicrotome. They were stained by uranyl acetate and lead citrate<sup>[12]</sup> and were examined by electron microscope in Electron Microscope Unit, Faculty of Science, Ain Shams University.

### Histomorphometric study and image analysis

1. Area percentage of green color (collagen fibers deposition) was estimated by use of Masson's trichrome stained sections.
2. Muscle thickness in micrometer:

Data were gained by use of a Leica Qwin 500 Image Analyzer Computer System (Cambridge, England, UK) at the Pathology Department, Faculty of Dental Medicine, Cairo University. Measurements were proceeded at ×400 magnification.

Values were collected for each parameter from six microscopic areas per slide, six slides per rat and six rats per group<sup>[13]</sup>.

### Statistical analysis

Statistical test was carried out by use of the SPSS software (Statistical Package for Social Studies- version 13.0) to measure the previous parameters. One-way analysis of variance (ANOVA) was utilized to match means in various groups with each other. Bonferroni Post Hoc test was utilized to reveal significance between every two individual groups.

The significance of the data was specified using the probability (*P. value*).  $P > 0.05$  was counted non-significant.  $P \leq 0.05$  was counted significant and  $P \leq 0.001$  was counted highly significant<sup>[14]</sup>. Data were given in tables and histograms, all set by using MS Excel 2013.

## RESULTS

### 1-Biochemical study

#### Serum levels of FT3

The serum levels of T3 were markedly higher in T3-treated senile group (group III) in comparison to senile rats (group II) and control adult group (group I) (Table 1).

#### Hyperglycemia and Insulin Resistance Results

Compared to adult group, senile rats displayed higher level of fasting insulin. Also, the fasting glucose was higher in senile versus adult group, although it was statistically insignificant. T3 administration in T3-aged rats decreased the levels of fasting insulin, fasting glucose compared to aged rats. All were statistically significant except for fasting glucose level (Table 1). In comparison to adult group fasting insulin levels were still significantly higher in T3-treated senile rats.

### 2. Histological study

#### Histological results of Hx&E stained sections

##### Group I (Adult Control group):

##### Light microscopic examinations:

The muscle showed three connective tissue layers: epimysium, Perimysium and endomysium. They were formed of dense irregular collagen fibers.

In Hx&E stained longitudinal sections, the epimysium, was the layer which covered the whole muscle, and consisted of dense irregular collagen fibers, from which the septa extended between the muscle bundles called Perimysium (Figure 1). Thin endomysium was demonstrated between the closely packed parallel muscle fibers (Figures 2,3). There were transverse striations of muscle fibers and the peripherally situated oval flat vesicular nuclei were seen. Fibrocytes were also seen in between skeletal muscle fibers (Figure 3). Transverse section of rat gastrocnemius muscle showed thin perimysium between the muscle fibers (Figure 4).

##### Group II (Senile):

##### Light microscopic examinations:

Thickened epimysium covered the damaged muscle bundles and associated with mononuclear inflammatory cell infiltrate together with few dilated blood vessels were seen (Figure 5). Some muscle fibers were thinned out with mononuclear cellular infiltrations in between them. Other muscle fibers appeared pale with loss of cross striations (Figures 6,7). Loss of continuity of some muscle fibers was detected. Some muscle fibers showed pale acidophilic homogenous area of cytoplasm and loss of striations. Deficient areas of muscle fibers were seen (Figure 7)

Thickened perimysium between the muscle bundles infiltrated with mononuclear inflammatory cell infiltrate specially around congested blood vessels were found (Figure 8). Multiple focal pale areas in intima of congested dilated blood vessels were seen. There was loss of architecture of muscle fibers in the form of disfigured muscle fibers with small dark pyknotic nuclei together with peripheral areas of degenerated cytoplasm were demonstrated (Figure 9). Splitting of muscle fibers with occasional fibrillation was noted. Occasional accumulation of fat cells in between the muscle fibers was noted. Areas of mononuclear inflammatory cellular infiltrations were seen (Figure 10).

##### Group III T3 Treated senile rats:

Light microscopic examinations: The epimysium was formed of dense regularly arranged collagen bundles covered the muscle fibers. Longitudinally arranged skeletal muscle fibers that appeared parallel to each other with well pronounced peripherally situated nuclei were seen. Muscle fibers were widely spaced with connective tissue (Figures 11,12). Transverse striations could be observed inside the muscle fibers (Figure 12).

#### Histological results of Masson's Trichrome stained sections

Transverse sections of the adult rats of control group I showed few thin collagen fiber depositions between the muscle fibers that appeared cylindrical or polygonal with peripheral nuclei (Figure 13). Transverse section of senile rat gastrocnemius muscle showed excessive collagen fibers deposition in between the disfigured muscle fibers and around the dilated and congested blood vessels associated with peripheral area of degenerated muscle fibers. (Figure 14). Transverse section of T3 treated senile group III gastrocnemius muscle showed few collagen fibers deposition in between muscle fibers (Figure 15).

#### Histological results of Toluidine blue stained semi-thin sections

Adult control rat gastrocnemius muscle showed muscle fibers with flattened nuclei beneath the sarcolemma sheath. The fibers showed transverse striations in the form of consecutive light and dark strips. The muscle fibers were separated by minimal connective tissue endomysium that contained blood vessels. The muscle fibers were nearly of uniform thickness (Figure 16). Semi-thin section of senile rat gastrocnemius muscle group II showed that the muscle fibers with different thickness together with area of discontinuity, loss of striations and loss of nuclei of some muscle fibers (Figure 17). Some muscle fibers either has pale nuclei with peripheral chromatin (Figure 18A) or pale nuclei (Karyolysis) and disturbed striations (Figure 18 B). Mononuclear inflammatory cell infiltrate in the connective tissue septa (endomysium) and around dilated congested blood vessel was noted. The muscle fibers displayed apparently different thickness and disturbed striations (Figure 19). Wide separation between the muscle fibers

was noticed with congested blood vessels in the thickened endomysium were observed. Many fibroblasts were seen between the muscle fibers together with macrophage cells (Figure 20). Thick walled blood vessels were noticed in the markedly thickened connective tissue septa in-between the muscle fibers. The mast cells were frequently encountered in the connective tissue septa with its characteristic metachromatic purple granules. Wide separation between the muscle fibers which were of different thickness was displayed (Figure 21).

Group III T3 treated senile rats showed normal spacing between muscle fibers in comparison with senile group II with thin endomysium in-between. The muscle fibers were nearly of uniform thickness and blood vessels were apparently normal (Figure 22)

**Histological results of Transmission Electron Microscopy (TEM) (Figures 23-30)**

TEM micrographs of the control adult group showed multiple adjacent sarcomeres with the cross-striations of myofibrils, dense Z line, light (I) band and dark (A) band bisected by M line and numerous oval mitochondria arranged parallel to the myofibrils between sarcomeres (Figure 23). Part of two muscle fibers with euchromatic nucleus beneath sarcolemma. Notice the regular arrangement of sarcomeres between two Z lines (Figure 24). TEM micrographs of the senile group showed marked disruption of the myofibrils (Z lines). Numerous large abnormally-shaped degenerated mitochondria, widening of the inter-fiber space with increased collagen fibers deposition were noted (Figures 25,26,27). Some fibers showed marked degeneration and vacuolations of the myofibrils with heterochromatic segmented invaginated nuclei that showed dense chromatin and peri-nuclear deposition of collagen fibers (Figure 28). The T3 treated senile group TEM micrographs showed restoration of the normal architecture of the myofibrils (Z lines), minimal vacuolations of sarcoplasm, numerous inter-myofibrillar longitudinally arranged mitochondria (Figure 29). Oval vesicular central nuclei with homogenous chromatin, peri-nuclear and inter-myofibrillar longitudinally arranged ovoid mitochondria were noted (Figure 30).

**Morphometric and statistical study**

Comparison between the average thicknesses of the muscle fibers in different groups was performed (Table 2, Histogram 1).

A statistically highly significant decrease in the average thickness of skeletal muscle fibers in group II (senile rats) compared to group I (adult rats). However, there were non-significant alterations in the mean thickness of skeletal muscle fibers in T3 treated senile rats (group III) in comparison to group I. Meanwhile, there was statistically highly significant increase in average thickness of skeletal muscle fibers in rats of group (III) in comparison to group (II).

Comparison between the area percentages of green color that represent the collagen fiber deposition in different groups was performed (Table 3, Histogram 2). A statistically highly significant increase in area percentage of green color for collagen fiber deposition was noticed in group (II) in comparison to that of group (I). However, non-significant alterations could be seen in the area percentage of green color for collagen fiber deposition in rats of group (III) relative to group (I). Meanwhile, there was statistically highly significant decrease in area percentage of green color for collagenous fibers deposition in rats of group (III) in comparison to group (II).

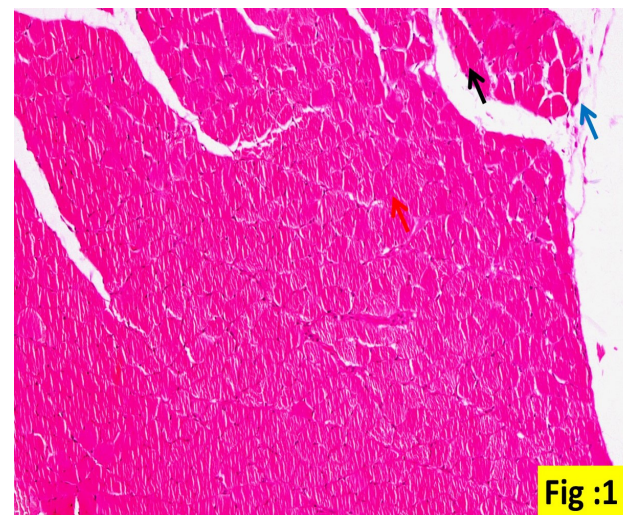


**Fig. 1:** A photomicrograph of a section of control adult rat gastrocnemius muscle group I showing thin epimysium (blue arrow) and perimysium (black arrow) surrounding bundles of muscle (red arrow).H and E X40

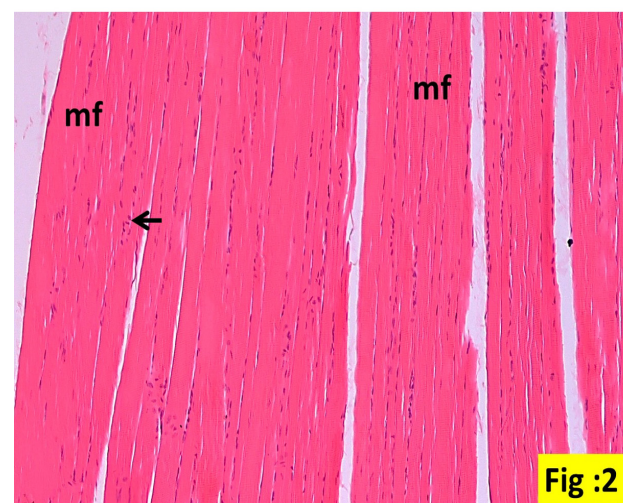


**Fig. 2:** A photomicrograph of a section of control adult rat gastrocnemius muscle group I showing parallel muscle bundles (mf) and thin endomysium (black arrow) between the closely packed individual muscle fibers. H and E X100

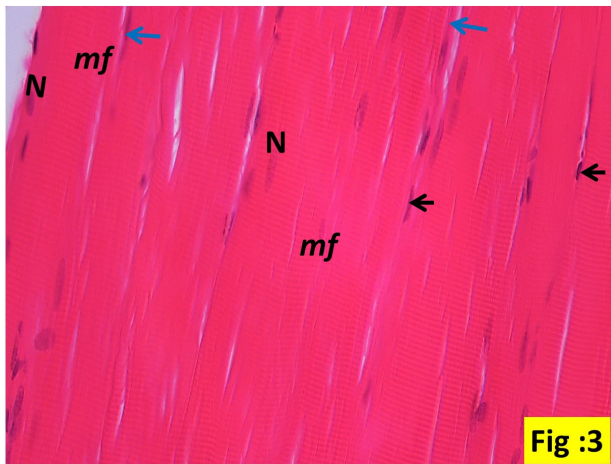


**Fig. 3:** A photomicrograph of a longitudinal section of control adult rat gastrocnemius muscle group I showing muscle fibers (mf). With the peripherally situated oval flat vesicular nuclei (N). Notice also the presence of fibrocytes in between skeletal muscle fibers (black arrow). Note also thin endomysium (blue arrow) between the individual muscle fibers H and E X400

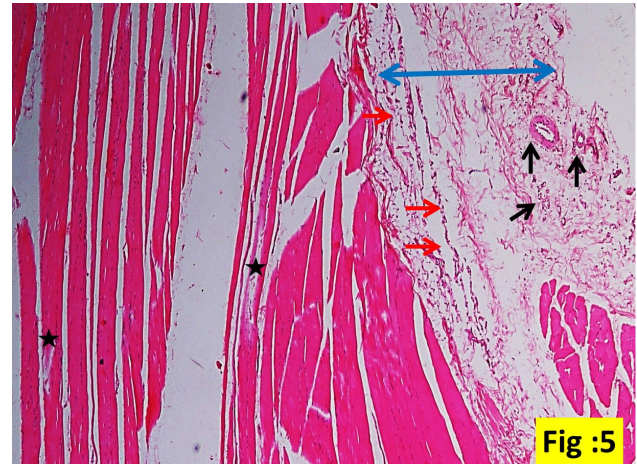


**Fig. 5:** A photomicrograph of a section of senile rat gastrocnemius muscle group II showing thickened epimysium (double head blue arrow) overlies the damaged muscle bundles (star) and note the presence of mononuclear inflammatory cell infiltrate (red arrow) in the epimysium together with few dilated blood vessels (black arrow). H and E X40

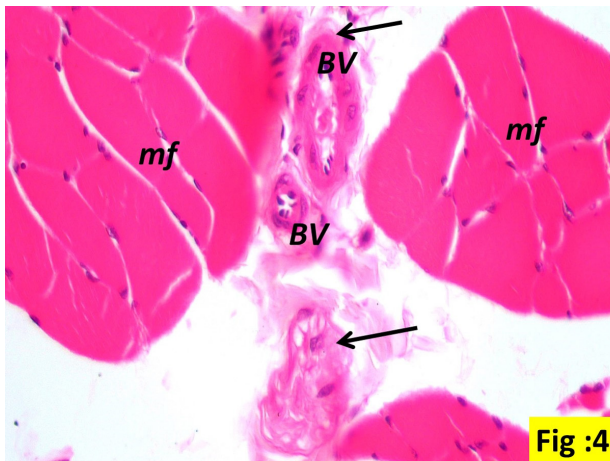


**Fig. 4:** A photomicrograph of a transverse section of control rat gastrocnemius muscle group I showing thin perimysium (black arrow) containing blood vessels (BV) between the muscle fibers(mf). H and E X 400

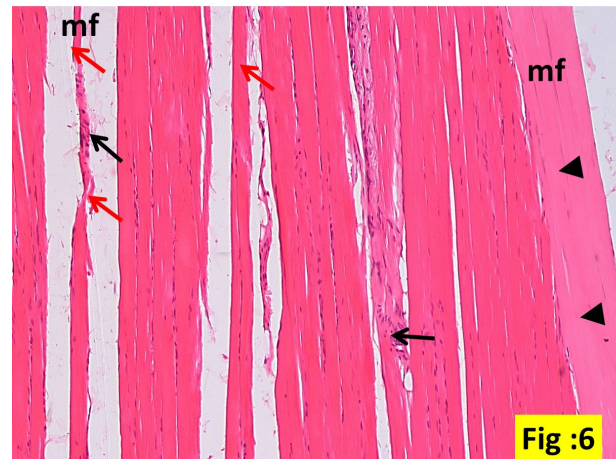


**Fig. 6:** A photomicrograph of a longitudinal section of senile rat gastrocnemius muscle group II showing apparent thinning out (red arrow) of some muscle fibers (mf) With mononuclear cellular infiltrations (black arrow) in between the muscle fibers. Some muscle fibers appear pale (arrow head). H and E X100

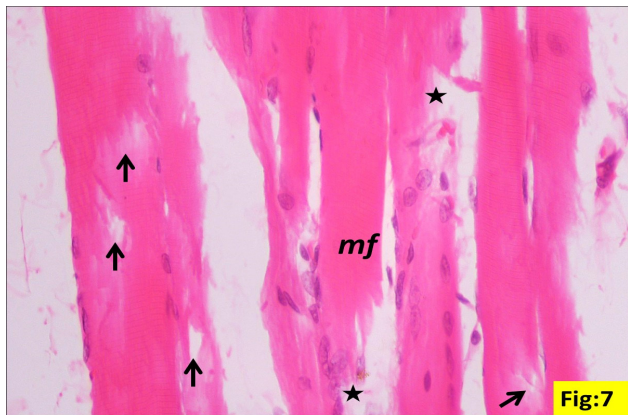


**Fig. 7:** A photomicrograph of a longitudinal section of senile rat gastrocnemius muscle group II showing loss of continuity (star) of some muscle fibers (mf), some muscle fibers show pale acidophilic homogenous area of cytoplasm (black arrow). H and E X400

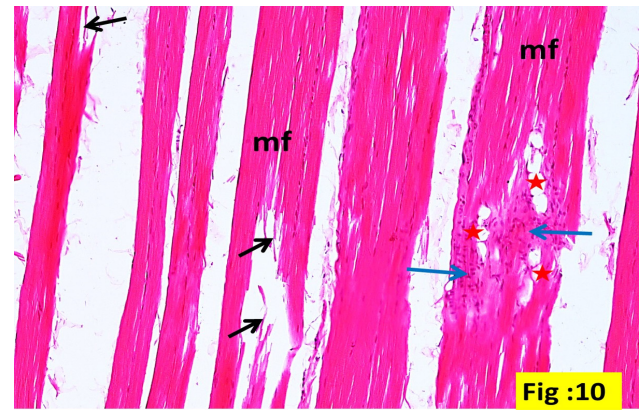


**Fig. 10:** A photomicrograph of a longitudinal section of senile rat gastrocnemius muscle group II showing splitting of muscle fibers (mf) with occasional fibrillation (black arrow). Occasional accumulation of fat cells (star) in between the muscle fibers is noted. Areas of mononuclear inflammatory cellular infiltrations (blue arrow) are seen. H and E X100

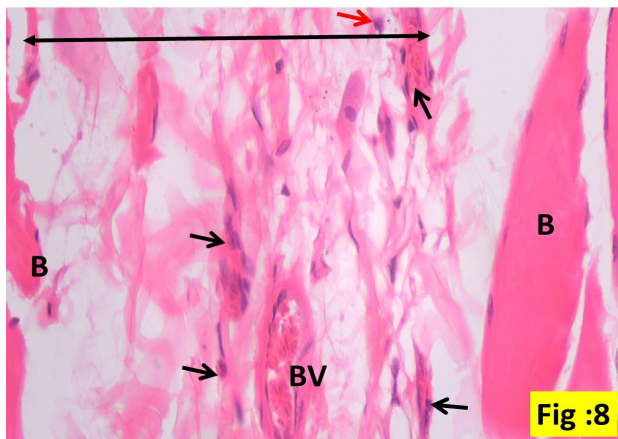


**Fig. 8:** A photomicrograph of a longitudinal section of senile rat gastrocnemius muscle group II showing apparently thickened perimysium (double head arrow) between the muscle bundles (B). Notice mononuclear inflammatory cell infiltrate (black arrow) around congested blood vessels (BV). H and E X400

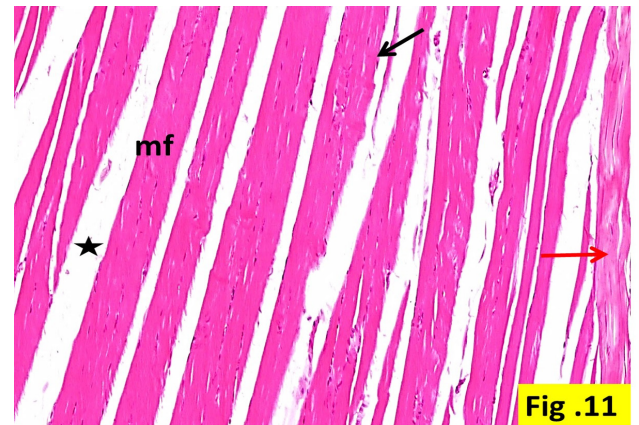


**Fig. 11:** A photomicrograph of a longitudinal section of rat gastrocnemius muscle of group III (senile treated with T3 for 2 weeks) showing epimysium (red arrow) formed of dense regularly arranged collagen bundles. Longitudinally arranged skeletal muscle fibers (mf) with well pronounced peripherally situated nuclei (black arrow) is seen. Notice the wide connective tissue spaces between the muscle fibers (star). H and E X40

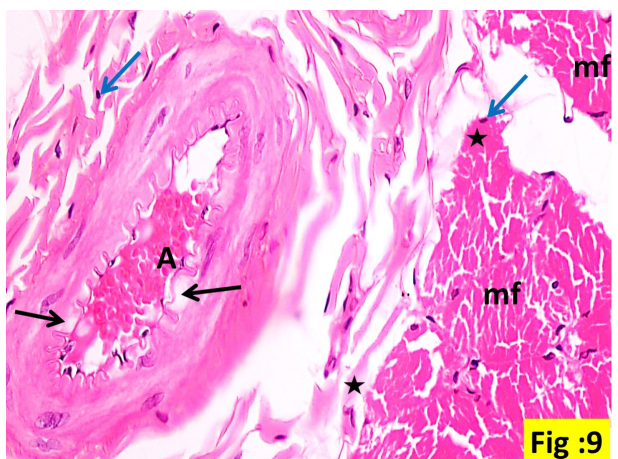


**Fig. 9:** A photomicrograph of a transverse section of senile rat gastrocnemius muscle group II showing loss of architecture of muscle fibers (mf). These distorted muscle fibers have small dark pyknotic nuclei (blue arrow) with peripheral areas of degeneration (star). Note multiple focal pale areas (black arrow) in intima of congested dilated artery (A). H and E X400

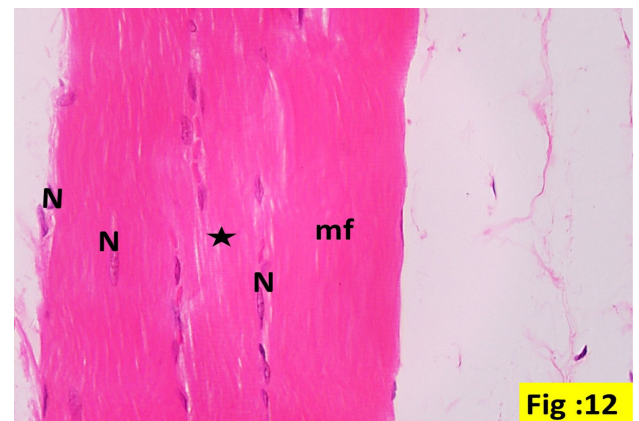


**Fig. 12:** A photomicrograph of a longitudinal section of rat gastrocnemius muscle of group III (senile treated with T3 for 2 weeks) showing regularly arranged skeletal muscle fibers (mf) with peripherally situated flat vesicular nuclei (N). Transverse striations can be observed inside the muscle fibers (star). H and E 400

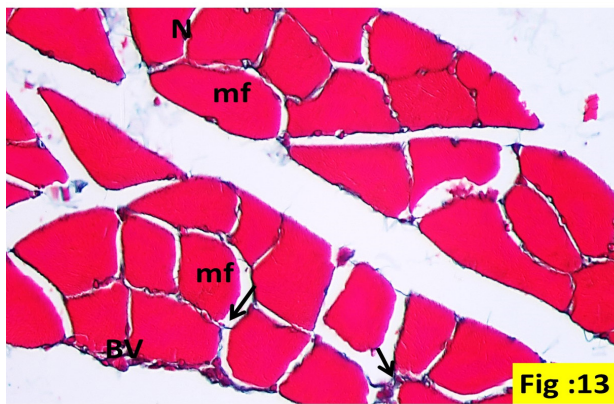


**Fig. 13:** A photomicrograph of a transverse section of gastrocnemius muscle of control adult rat group I showing thin collagen fiber (black arrow) deposition between muscle fiber (mf) that appear cylindrical or polygonal in shape with flattened peripheral nuclei (N). BV=blood vessels Masson's trichrome X400

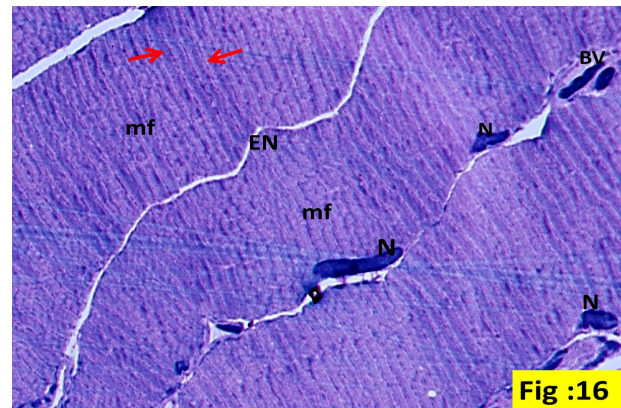


**Fig. 16:** A photomicrograph of a semi-thin section of control adult rat gastrocnemius muscle group I showing myofibers(mf) with flattened nuclei(N) beneath the sarcolemma sheath. The fibers showed transverse striations in the form of alternating dark and light bands (red arrow). The muscle fibers are separated by minimal connective tissue endomysium (EN) that contains blood vessels(BV). Toluidine blueX1000

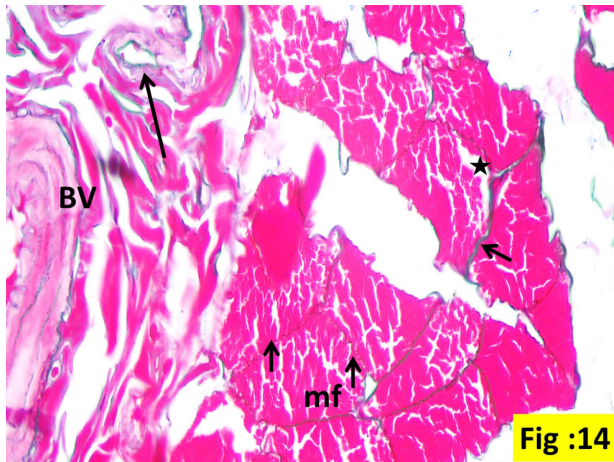


**Fig. 14:** A photomicrograph of a transverse section of senile rat gastrocnemius muscle group II showing apparent increase in the collagen fiber deposition (black arrow) in between the disfigured muscle fibers (mf) that reveal peripheral area of degeneration (star). Notice also excessive collagen fiber deposition around the dilated congested blood vessels (BV). Masson's trichrome X400

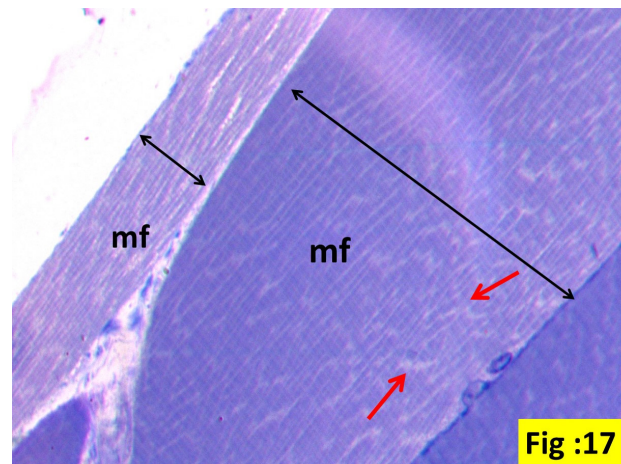


**Fig. 17:** A photomicrograph of a semi-thin section of senile rat gastrocnemius muscle group II showing the muscle fibers (mf) with apparently variable thickness (↑) together with disturbed striations (red arrow) and loss of nuclei of some muscle fibers. Toluidine blue X1000

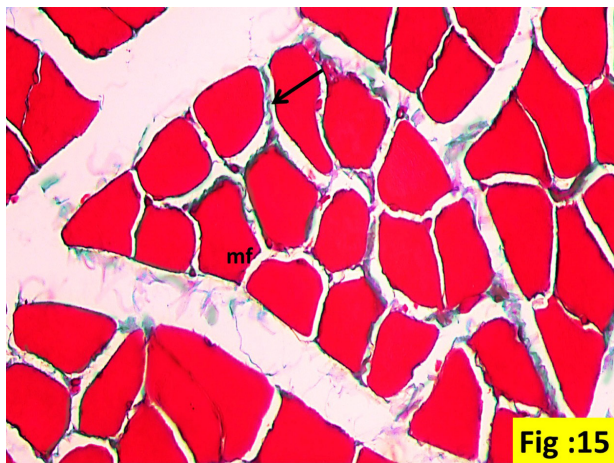


**Fig. 15:** A photomicrograph of a transverse section of group III (senile treated with T3 for 2 weeks) showing minimal collagen fibers deposition (black arrow) in between muscle fibers (mf). Masson's trichrome X400

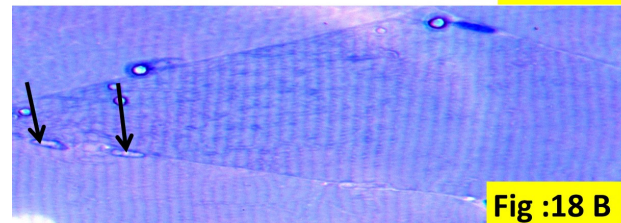
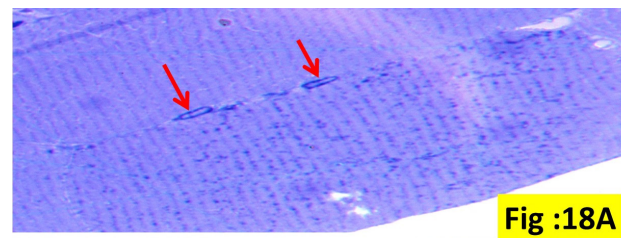


**Fig. 18:** A photomicrograph of a semi-thin section of senile rat gastrocnemius muscle group II showing some muscle fibers has either pale nuclei with peripheral chromatin (red arrow) (18A) or dissolution of nuclear material (Karyolysis) (black arrow) (18B). Toluidine blueX1000

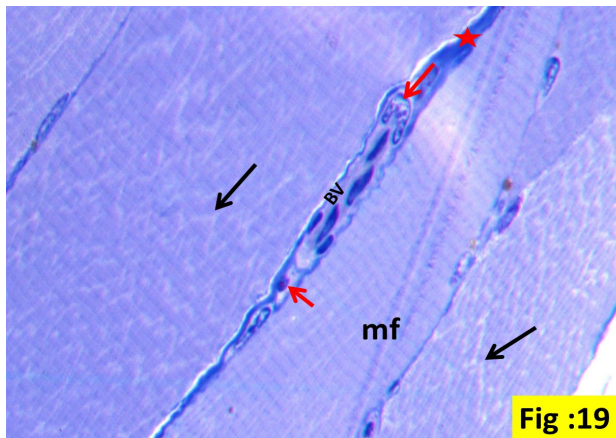


Fig :19

Fig. 19: A photomicrograph of a semi-thin section of senile rat gastrocnemius muscle group II showing mononuclear inflammatory cell infiltrate (red arrow) in the connective tissue septa (endomysium) (star) in close proximity to congested dilated blood vessel (BV). Note that the myofibrils (mf) showed disturbed striations (black arrow). Toluidine blueX1000

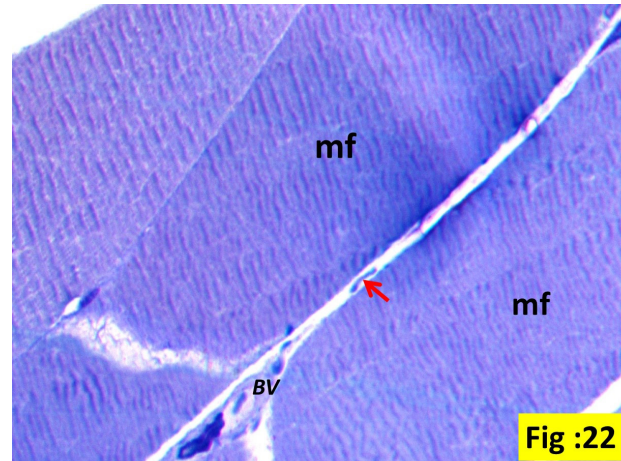


Fig :22

Fig. 22: A photomicrograph of a section of gastrocnemius muscle group III (T3 treated senile for 2 weeks) showing normal spacing between muscle fibers (mf) with thin endomysium (red arrow) in between. The muscle fibers and blood vessels (BV) are apparently normal. Toluidine blue X 1000

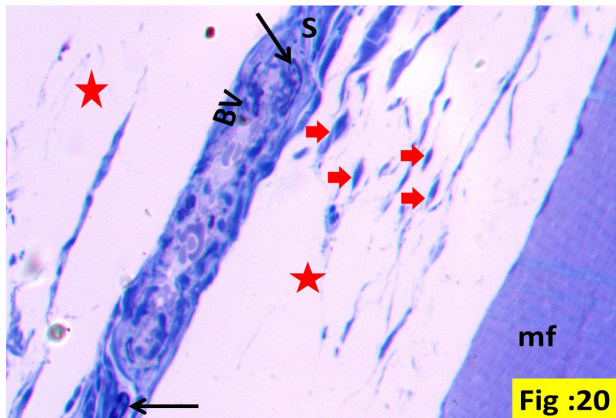


Fig :20

Fig. 20: A photomicrograph of a semi-thin section of senile rat gastrocnemius muscle group II showing wide separation (star) between the muscle fibers (mf) with congested blood vessels (BV) in the thickened connective tissue septa(S) (endomysium). Notice many fibroblasts are seen between the muscle fibers (red short arrow). (Black arrow) = macrophage cells. Toluidine blueX1000

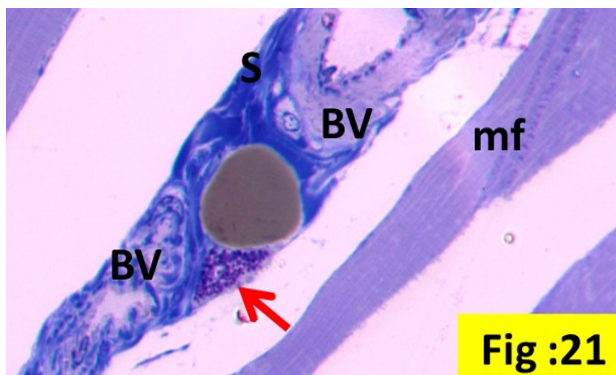


Fig :21

Fig. 21: A photomicrograph of a semi-thin section of senile rat gastrocnemius muscle group II showing thick walled blood vessels (BV) in the markedly thickened connective tissue septa(S) between the muscle fibers(mf). Note the mast cells (red arrow) that are frequently encountered in the connective tissue septa with its characteristic metachromatic purple granules. Toluidine blueX1000

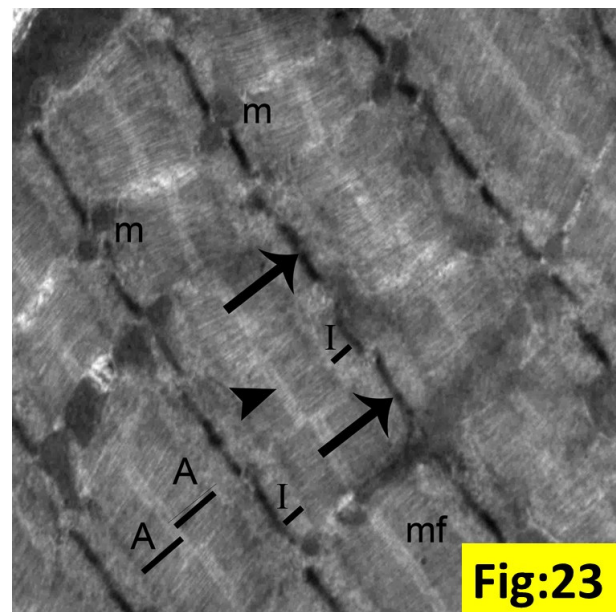
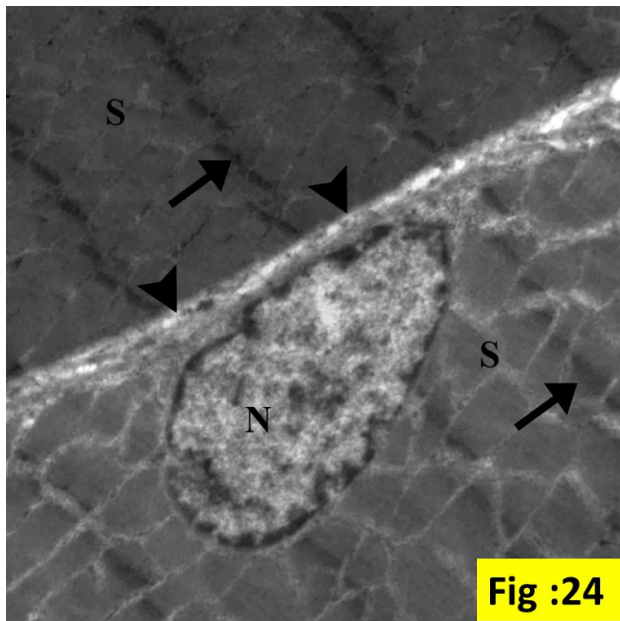


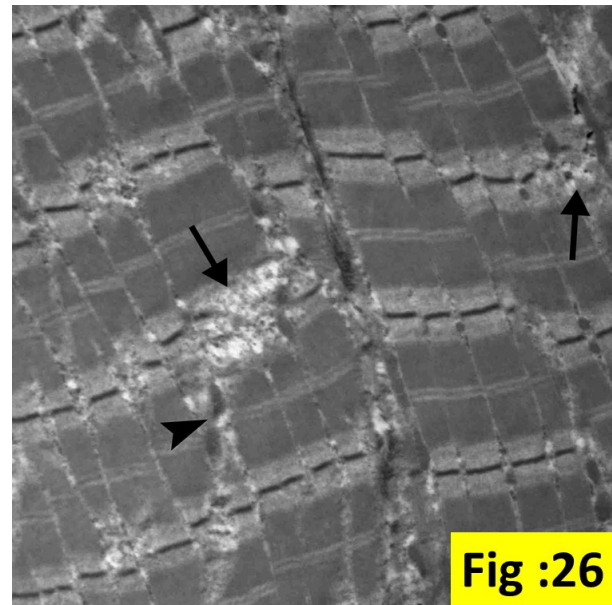
Fig:23

Fig. 23: Transmission electron micrograph of a section of rat gastrocnemius muscle (control adult group) showing cross striations of myofibrils (mf): dense Z line (arrow); light (I) band and dark (A) band bisected by M line (arrowhead). Mitochondria (m) are arranged parallel to myofibrils between sarcomeres. Uranyl acetate and Lead Citrate X 5000



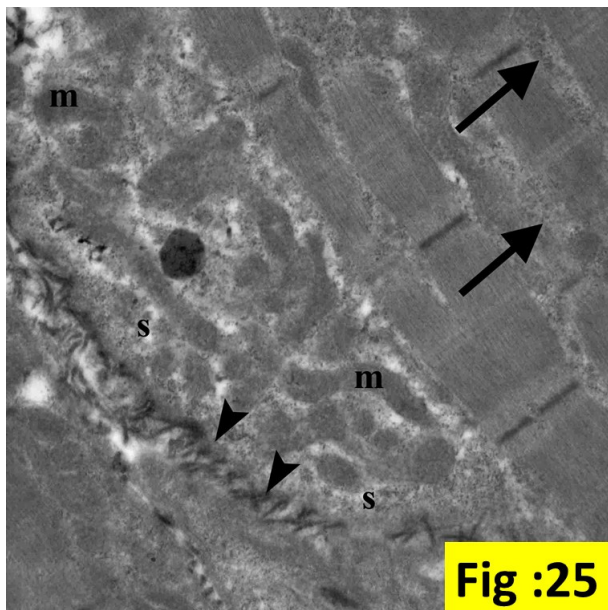
6.jpg  
2 μm  
HV=100.0kV  
Direct Mag: 3000x  
X:na Y:na T:

**Fig. 24:** Transmission electron micrograph of a section of rat gastrocnemius muscle (control adult group). Part of two muscle fibers with euchromatic nucleus (N) beneath sarcolemma (arrowhead). Notice the regular arrangement of sarcomeres(S) between two intact Z line (arrow). Uranyl acetate and Lead Citrate X 3000



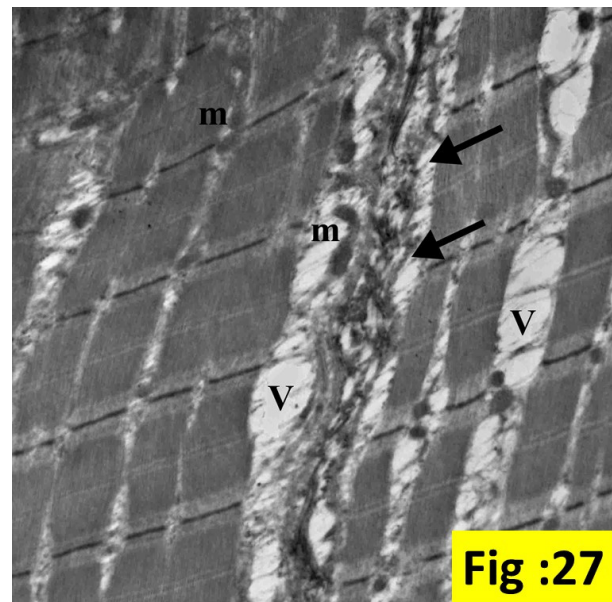
5.jpg  
2 μm  
HV=100.0kV  
Direct Mag: 3000x  
X:na Y:na T:

**Fig. 26:** Transmission electron micrograph of a section of rat gastrocnemius muscle (senile group) showing disruption of the myofibrils Z line (arrow) and degenerated mitochondria (arrowhead). Uranyl acetate and Lead Citrate X3000



2.jpg  
500 nm  
HV=100.0kV  
Direct Mag: 6000x  
X:na Y:na T:

**Fig. 25:** Transmission electron micrograph of a section of rat gastrocnemius muscle (senile group) showing disruption and disorganization of the myofibrils Z line (arrow): abnormally shaped degenerated mitochondria (m) and widening of the inter-fiber spaces (s) with excessive deposition of collagen fibers (arrowhead). Uranyl acetate and Lead Citrate X 6000



6.jpg  
2 μm  
HV=100.0kV  
Direct Mag: 3000x  
X:na Y:na T:

**Fig. 27:** Transmission electron micrograph of a section of rat gastrocnemius muscle (senile group) showing excessive vacuolations (V) of the myofibrils Z line, widening of inter-fiber spaces with excessive deposition of collagenous fibers (arrow). Abnormal shapes of mitochondria (m) are also seen. Uranyl acetate and Lead Citrate X 3000

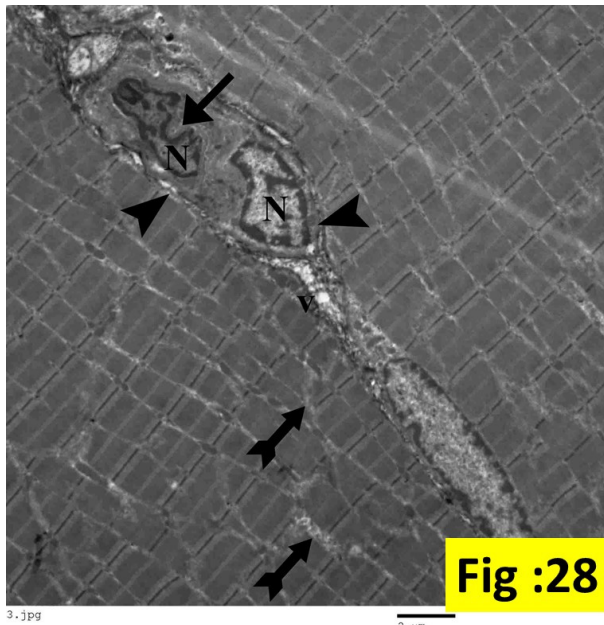


**Fig. 28:** Transmission electron micrograph of a section of rat gastrocnemius muscle (senile group) with the myofibrils Z line showing degeneration (tailed arrow) and vacuolations (v). Segmented nucleus (N) shows invaginations (arrow) with condensed heterogeneous chromatin and perinuclear deposition of collagen fibers (arrowhead). Uranyl acetate and Lead Citrate X 1500

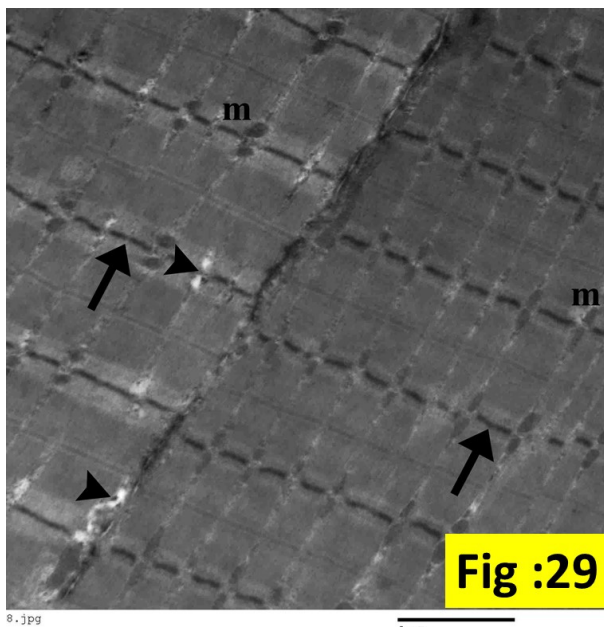


**Fig. 29:** Transmission electron micrograph of a section of rat gastrocnemius muscle (T3-treated senile group) showing restoration of the normal architecture of the myofibrils with intact Z line (arrow); minimal vacuolations (arrowhead) of sarcoplasm, longitudinally arranged mitochondria (m) parallel to myofibrils. Uranyl acetate and Lead Citrate X 3000

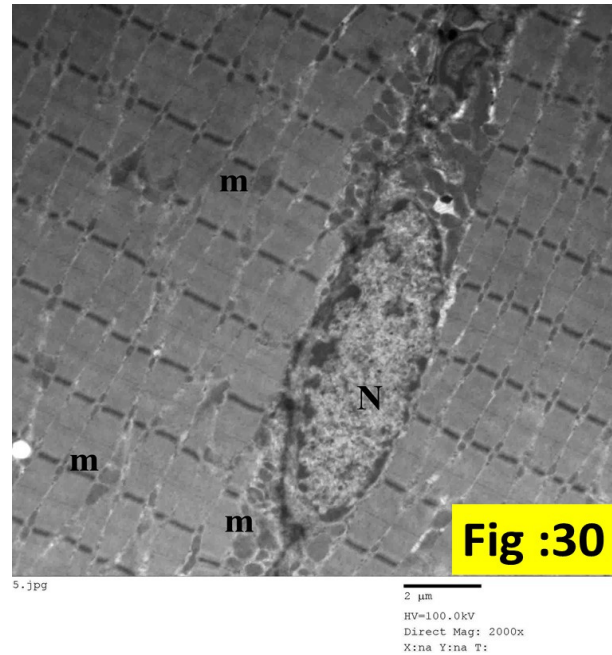
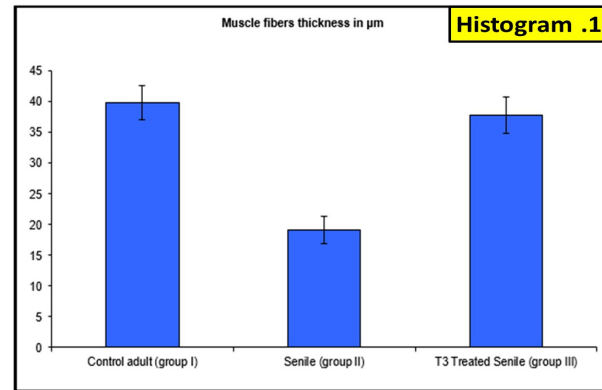
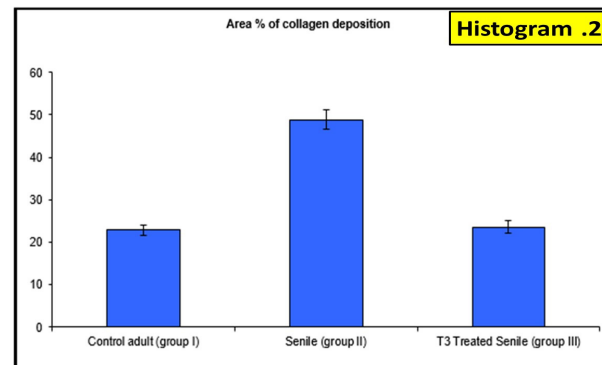


**Fig. 30:** Transmission electron micrograph of a section of rat gastrocnemius muscle (T3-treated senile group) showing oval nucleus (N) with homogenous chromatin, numerous mitochondria (m) parallel to the myofibrils and in the perinuclear space. Uranyl acetate and Lead Citrate X 2000



**Histogram 1:** Showing the difference in muscle fibers thickness in μm among different groups.



**Histogram 2:** Showing the difference in Area % of collagen deposition among the three different groups

**Table 1:** serum levels of free triiodothyronine (FT3), fasting glucose, fasting insulin, in the three study groups.

	Groups		
	adult	senile	T3-treated senile
FT3 (ng/dl)	2.93±0.1	2.41 ± 0.3	3.1± 0.5#
Fasting glucose (mg/dl)	94.9 ±4.9	104.9±12.8	94.8 ±2.9
Fasting insulin (mg/dl)	1.29±0.3	1.83±0.1*	1.59±0.9*#

Data are expressed as mean ± SD, n = 7 per each group; \*  $p < 0.05$  vs. adult group, #  $p < 0.05$  vs. senile group. T3- triiodothyronine-treated senile group

**Table 2:** Showing the difference in muscle fibers thickness in  $\mu\text{m}$  among different groups.

Muscle fibers thickness in $\mu\text{m}$	Control adult (group I)	Senile (group II)	T3 Treated Senile (group III)	One Way ANOVA test		
	No. = 6	No. = 6	No. = 6	F	P-value	Sig.
Mean ± SD	39.9 ± 2.75	19.1 ± 2.19	37.8 ± 2.971	111.408	<0.001	HS
Post Hoc analysis by LSD						
	Control Vs Senile		Control Vs treated Senile		Senile Vs T3 treated Senile	
	<0.001 (HS)		0.233 (NS)		<0.001 (HS)	

SD = standard deviation.

$P$  value < 0.05 = significant (S).

$P$  value < 0.01 = highly significant (HS).

$P$  value > 0.05 = non-significant (NS).

**Table 3:** Showing the difference in Area % of collagen deposition among the three different groups.

Area % of green color (collagen deposition)	Control adult (group I)	Senile (group II)	T3 Treated Senile (group III)	One Way ANOVA test		
	No. = 6	No. = 6	No. = 6	F	P-value	Sig.
Mean ± SD	22.93 ± 1.2	48.9 ± 2.3	23.58 ± 1.5	439.632	<0.001	HS
Post Hoc analysis by LSD						
	Control Vs Senile		Control Vs treated Senile		Senile Vs treated Senile	
	<0.001 (HS)		0.427 (NS)		<0.001 (HS)	

SD = standard deviation.

$P$  value < 0.05 = significant (S).

$P$  value < 0.01 = highly significant (HS).

$P$  value > 0.05 = non-significant (NS).

## DISCUSSION

Skeletal muscle maintains erect position and helps in movement by contributing to basal energy metabolism. Thyroid hormones (triiodothyronine, or T3) participate in contractile function, metabolic processes, myogenesis and regeneration of skeletal muscle. During aging skeletal muscle presents a decrease in its mass termed Sarcopenia. There is a great confirmation that thyroid hormones have a great value in modulating the sarcopenic process. Therefore, in this study, we aimed to discuss the protective effects of thyroid hormones in skeletal muscular aging processes and myopathy-related to aged associated thyroid dysfunction<sup>[15,16,17]</sup>

Gastrocnemius (GAS) muscle is chiefly formed of type II (fast twitch) fibers<sup>[15]</sup> that markedly diminished with advancing age<sup>[16]</sup>. Furthermore, in senile age, GAS showed marked increase in apoptosis. This agreed with results of the present study, in both the H&E-stained sections and the toluidine blue stained semi thin sections of senile group, that showed nuclear pyknosis and disturbed

striations of muscle fibers. Aging caused muscle atrophy mainly through affecting type II fibers<sup>[17]</sup>. Up-regulation of cell death-inducing DNA fragmentation factor alpha like effector A (CIDEA) in GAS with age resulted in significant decrease in its mass<sup>[18]</sup>.

In the current study, H&E-stained sections of gastrocnemius muscle of senile rats showed damaged muscle bundles, thinning out of some muscle fibers, deficient areas and loss of architecture of muscle fibers.

Muscle atrophy with old age is mainly due to intrinsic apoptotic pathway that is different between slow and fast-twitch muscle<sup>[19]</sup>. Caspase-9; a key molecule in the intrinsic apoptotic pathway, were significantly up-regulated in fast-twitch muscle by aging<sup>[20]</sup>.

In the present study, the morphometric results of senile rats showed statistically significant decrease in the muscle thickness, this was explained by some authors, who showed that optic atrophy 1 (OPA1) was markedly reduced in the skeletal muscles (SM) of senile mice and that exact hit of OPA1 in SM inhibited protein synthesis, promoted protein

breakdown, and induced atrophy-linked gene expression, causing early aging changes in mice<sup>[21]</sup>.

Furthermore, in the present study, the morphometric results of senile rats showed statistically significant increase in the collagen fiber deposition inbetween the muscle bundles in the Masson's Trichrome stained sections, this was explained by many studies which stated that OPA1 lack promoted the release of Fibroblast Growth Factor 21 (FGF21) from SM, causing changed lipid homeostasis, inflammation, and the senility of various tissues<sup>[22]</sup>. These findings explained and justified the results of the present study in the H&E stained sections of senile group that presented mononuclear inflammatory cell infiltrate between muscle fibers and in the epimysium in addition to fat cell accumulation in between the muscle fibers together with congested dilated blood vessels of the perimysium and endomysium. Moreover, <sup>[22]</sup> findings explained and were in consistence with the results of the present study, seen in the toluidine blue stained semi thin sections of senile group that showed mast cells one of recruited inflammatory cells with its characteristic purple metachromatic granules in between the muscle fibers.

Furthermore, some studies proved that the GAS muscles of senile rats displayed markedly increased dynamin-related protein 1 (DRP1)<sup>[23]</sup>. They evidenced that precise overexpression of DRP1 in skeletal muscle led to mitochondrial network reformation and diminished mitochondrial DNA copy number. Also, stimulated dsRNA-dependent protein kinase/eukaryotic initiation factor 2/fibroblast growth factor 21 pathway via Drp1 overexpression caused diminished SM protein production<sup>[24]</sup>. This fact was explained and agreed with results of the present study that were seen in the Masson trichrom's stained sections of senile group that demonstrated increased irregular thickened collagen fibers deposition inbetween the damaged muscle fibers and around the dilated congested blood vessels. Which was confirmed by the morphometric results of the current work, in the senile rats group II that showed statistically significant increase in the collagen fiber deposition.

In the current study, H&E-stained sections of gastrocnemius muscle of senile rats (group II) showed degeneration of the intima of the wall of the blood vessels in-between the muscle fibers in the form of focal pale area of the intimal wall. These consequences agreed with many studies on rodents, they stated that, among age-related diseases, cardiovascular and cerebrovascular diseases which are the major causes of death. Vascular dysfunction is a primary feature of these diseases and main risk factor. They demonstrated that there were morphological aberrations of aging vessels, which includes senile microvessel damage, altered capillary basement membrane, intima, media, adventitia as well as accompanying vascular dysfunctions due to these changes<sup>[25]</sup>. These results were explained by endothelial apoptosis and senescence in rat's peripheral blood vessels<sup>[26]</sup>. They added that the electron microscopy reveals deposition of connective tissue in the intima below the endothelium.

Ultrastructural examination of gastrocnemius muscle in senile rats showed marked disruption of the myofibrils (z lines) with loss of architecture of the muscle fiber, numerous large abnormally shaped degenerated mitochondria, widening of the inter-fiber space with rise in collagenous fibers deposition. Some fibers showed marked degeneration and vacuolations of the myofibrils with heterochromatic segmented invaginated nuclei showing dense chromatin and peri-nuclear deposition of collagen fibers. These outcomes agree with studies describing that aging of SM resulted in oxidative stress and mitochondrial dysfunction<sup>[27]</sup>. GAS was considered a glycolytic white muscle that showed mitochondrial elongation in senile rats<sup>[18]</sup>, associated with enlarged SM mitochondria<sup>[28]</sup>, more branching and morphological convolution of mitochondria<sup>[29]</sup> and rise in mitochondrial fusion<sup>[30]</sup>.

Aging is related to sarcopenia; a progressive decrease of muscle mass and force. Advancing age is connected with both obesity and insulin resistance (IR) in humans and rodents<sup>[31]</sup>. SM is the chief site of insulin action, so it is essentially related to the progress of whole-body insulin resistance<sup>[32]</sup>. SM has a main role in the insulin resistance development all-over the body<sup>[33]</sup>. Mitochondria are the main determinants of the IR progress<sup>[34]</sup>. Senile rats showed diminished activities of SM mitochondria<sup>[35]</sup>. Also, old men showed mitochondrial dysfunction<sup>[36]</sup>. Furthermore, SM insulin sensitivity and oxidative capacity were directly related<sup>[37]</sup>. Mitochondrial dysfunction contributed to the advance of insulin resistance<sup>[36]</sup>, and mitochondrial oxidative capability was an excellent anticipator of insulin sensitivity<sup>[37]</sup>.

Mitochondrial dysfunction was evidenced to cause sarcopenia mostly due to altered mitochondrial dynamics/morphology<sup>[18]</sup>. Mitochondria supply energy for skeletal muscle contraction via oxidative phosphorylation (OXPHOS). Also, mitochondria are essential for skeletal muscle cell viability and redox elimination. Mitochondria were described as multifunctional indicator centers that link cellular task with metabolism and age<sup>[38]</sup>. Mitochondria are essential for cellular homeostasis in response to extracellular and intracellular strain and aging. Mitochondrial dysfunction is a characteristic of aging<sup>[39]</sup>. With ageing, functional changes emerge in skeletal muscle mitochondrial function, namely; decreased membrane potential, increased ROS production, altered enzyme activity, and decreased adenosine triphosphate (ATP) production ability<sup>[40]</sup>. Therefore, to improve function of skeletal muscle cell and delay aging, mitochondrial function regulation is considered an essential factor<sup>[41]</sup>. With aging, skeletal muscles display a decrease in mitochondrial number, density, mitochondrial protein expression and mitochondrial deoxyribonucleic acid (DNA) copy number<sup>[40]</sup>.

The present work demonstrated the hormonal profile of senile rats in comparison to adult rats. The aged rats presented statistically significant higher levels of fasting insulin in addition to statistically insignificant higher

fasting glucose (Table 1), this was explained by researchers who stated that about 80% of glucose is consumed by skeletal muscle in mice (SM) in response to insulin; then oxidized to supply energy or stored as glycogen<sup>[42]</sup>. SM are essential insulin-responsive tissues<sup>[43]</sup>. Peroxisome proliferator-activated receptor  $\gamma$  coactivator-1 $\alpha$  (PGC-1 $\alpha$ ) is a primary gene controlling skeletal muscle insulin sensitivity and mitochondrial biogenesis. Skeletal muscle of senile mice displayed decreased PGC-1 $\alpha$ . PGC-1 $\alpha$  overexpression in the senile mice skeletal muscle caused increased skeletal muscle mitochondrial number, renewal of myosin heavy chain isoforms, elevated mitophagy (precise type of autophagy selectively eliminates damaged mitochondria via the autophagy-lysosome system) markers and minimized levels of proteasome markers, and these alterations simulated the molecular characteristics of young mouse SM<sup>[44,45]</sup>. Disturbed mitophagy with uneven mitochondrial dynamics caused gathering of dysfunctional mitochondria in senility<sup>[44]</sup>. SM of old rodents displayed decreased mitophagy-related proteins with accumulation of dysfunctional mitochondria<sup>[29,46]</sup>.

Many researches evidenced that PGC-1 $\alpha$  overexpression in SM of 24-month-old male mice minimized muscle weakness and stopped sarcopenia<sup>[47]</sup>. In aging SM, the mitochondrial quality regulating system is disrupted, including diminished mitochondrial biogenesis, an disproportionate mitochondrial dynamics, and worsened mitophagy<sup>[48]</sup>. Therefore, regulating the mitochondrial biogenesis represents a probable step to prevent skeletal muscle aging.

Nr1d1 (known as Rev-erb- $\alpha$ ) is positively correlated to mitochondrial tasks and oxidative capability in SM. Nr1d1 expression is diminished in senile SM. Nr1d1 overexpression augments mitochondrial function and exercise ability<sup>[49]</sup>. In contrast, the shortage of Nr1d1 in SM upregulated the atrophy related genes and increased sarcopenia<sup>[50]</sup>.

In senile humans and rodents mitochondrial permeability transition pore (mPTP) dysfunctions leading to the aging-related sarcopenia, since mPTP opening can initiate numerous atrophy-regulating pathways<sup>[51]</sup>, via overproduction of mitochondrial reactive oxygen species (ROS)<sup>[52]</sup>. ROS can initiate the muscle atrophy course by stimulating the Fork head box O (FoxO) transcription factor family<sup>[53]</sup>. Also, mPTP opening can release mitochondrial DNA and consequently activates the NLRP3 (NOD-, LRR- and pyrin domain-containing protein 3) inflammasome, that increases the expression of ubiquitin ligases concerned with muscle atrophy<sup>[54]</sup>. Meanwhile, mPTP opening releases cytochrome C that increases proteasomal action secondary to caspase 3 stimulation<sup>[55]</sup>. Lastly, mPTP opening can release pro-apoptotic agents such as endonuclease G, that accumulates in myonuclei of senile individuals<sup>[51]</sup>. Furthermore, overexpression of the antioxidant enzyme; mitochondrial-targeted catalase diminishes sarcopenia occurring with senility.

In the present study, the H&E stained sections and semi thin sections of group III (T3 treated senile group) showed marked restoration of the normal architecture of the muscle fibers with regularly arranged collagen bundles, longitudinally arranged skeletal muscle fibers and peripherally situated nuclei. This agreed with scientists who stated that in SM, T3 augments glucose uptake and both glycolytic and oxidative capability<sup>[56]</sup>. This was explained many authors who described that T3 fulfills its effects via connecting with TH receptor (TR)<sup>[57]</sup>. T3 promptly increases transcriptional coactivator PGC1 $\alpha$ ; peroxisome proliferator-activated receptor  $\gamma$  (PPAR $\gamma$ ) coactivator 1 $\alpha$  (PGC1 $\alpha$ ), encoded by PPARGC1A<sup>[57,58]</sup>. SM displays high expression of PGC1 $\alpha$ <sup>[59]</sup>. In SM, it induces mitochondrial biogenesis, encourages switch from glycolytic to oxidative fibers, and improves fatigue resistance<sup>[59]</sup>. This agreed with ultrastructural findings in the thyroid hormone treated group (group III) in the present study that showed muscle fibers; nearly of uniform diameter, with restoration of the normal architecture of the myofibrils (z lines), minimal vacuolations of sarcoplasm, numerous inter-myofibrillar longitudinally arranged mitochondria, oval vesicular central nuclei with homogenous chromatin, peri-nuclear and inter-myofibrillar longitudinally arranged ovoid mitochondria. Mitochondria have a chief role in insulin resistance. SM insulin resistance often ensues due to mitochondrial dysfunction<sup>[60]</sup>.

Morphometric results in the present investigation of group III (T3 treated senile group), showed statistically significant increase in the muscle thickness. This was explained by Milanese *et al.*,<sup>[61]</sup> who stated that TH signaling via TR $\alpha$ 1 is vital to preserve muscle satellite cell collection, important for appropriate muscle regeneration and to compete sarcopenia.

In the present study, the hormonal profile of group III (T3 treated senile group), showed that T3 administration decreased the levels of fasting insulin and fasting glucose compared to senile rats. This agreed with Moreno *et al.*,<sup>[1]</sup> who stated that glucose uptake was improved by providing T2 (a naturally occurring iodothyronine, 3,5-diiodo-L-thyronine) to muscle cells, and consequently it improved insulin sensitivity. T2 significantly stimulated insulin-induced Akt, that is concerned with glucose transport and glycogenesis in SM cells<sup>[62]</sup>. Furthermore, it was responsible for muscle hypertrophy *in vivo*<sup>[63]</sup>. Similarly, other workers, produced obese Akt1 transgenic mice that showed fast/glycolytic muscle fibers, and consequently growth of these muscle fibers settled their reactions to exogenous glucose and insulin<sup>[64]</sup>.

So that, TH effect in SM is a significant factor; linked to insulin sensitivity. T3 affects metabolic paths which impede insulin action<sup>[65]</sup>.

Furthermore, SM display a key T3-responsive gene; ATP2A2, that encodes sarcoplasmic reticulum Ca<sup>2+</sup>-dependent ATP-ase (SERCA) 2 $\alpha$ , an isoform for SM fibers, manifested by greater insulin sensitivity<sup>[66]</sup>. Serum TSH

and insulin sensitivity were inversely related with a decline in serum fT4 in overweight/obese individuals<sup>[32]</sup>. Thyroid hormones altered gene expression and enzymatic activities linked to glucose metabolism & insulin sensitivity<sup>[5]</sup>.

### CONCLUSION

The present study proved that thyroid hormone supplementation to old aged rats in situations with low serum T3 level can improve the structural abnormalities encountered in gastrocnemius muscle that were mostly due to low T3 and diminished insulin sensitivity found in old aged rats. This improvement by T3 was achieved through many mechanisms as T3 improved the insulin sensitivity and glucose uptake by the skeletal muscle through its effect on mitochondria and its linked enzymes.

### RECOMMENDATIONS

It's advised to give T3 supplementations for those elderly in situations with low serum T3 level and complaining from Sarcopenia and glucose intolerance.

### CONFLICT OF INTERESTS

There are no conflicts of interest.

### REFERENCES

- Moreno M, Silvestri E, De Matteis R, de Lange P, Lombardi A, Glinni D, Senese R, Cioffi F, Salzano A, Scaloni A, Lanni A, and Goglia F. 3,5-Diiodo-L-thyronine prevents high-fat-diet-induced insulin resistance in rat skeletal muscle through metabolic and structural adaptations. *FASEB Journal: Official Publication of the Federation of American Societies for Experimental Biology*, (2011) 25(10): 3312–3324, DOI: 10.1096/fj.11-181982.
- Akintola AA, van Heemst D. Insulin, aging, and the brain: mechanisms and implications. *Front Endocrinol (Lausanne)*. (2015) 6:13. <https://doi.org/10.3389/fendo.2015.00013>.
- El Agaty MS. Triiodothyronine improves age-induced glucose intolerance and increases the expression of sirtuin-1 and glucose transporter-4 in skeletal muscle of aged rats *Gen. Physiol. Biophys.* (2018) 37: 677–686. DOI: 10.4149/gpb\_2018026
- Mohamed JS, Wilson JC, Myers MJ, Sisson KJ, Alway SE. Dysregulation of SIRT-1 in aging mice increases skeletal muscle fatigue by a PARP-1-dependent mechanism. *Aging (Albany NY)* (2014) 6: 820–834. DOI: 10.18632/aging.100696
- Giacco A, Delli Paoli G, Senese R, Cioffi F, Silvestri E, Moreno M, Ruoppolo M, Caterino M, Costanzo M, Lombardi A, Goglia F, Lanni A, and de Lange P. The saturation degree of fatty acids and their derived acylcarnitines determines the direct effect of metabolically active thyroid hormones on insulin sensitivity in skeletal muscle cells. *FASEB Journal: Official Publication of the Federation of American Societies for Experimental Biology* (2019) 33(2): 1811–1823. DOI: 10.1096/fj.201800724R
- Brenta G. Diabetes and thyroid disorders. *Br. J. Diabetes vasc. Dis.* (2010) 10: 172–177. <https://doi.org/10.1177/1474651410371321>
- Biondi B, Kahaly GJ, Robertson RP. Thyroid Dysfunction and Diabetes Mellitus: Two Closely Associated Disorders. *Endocr Rev.* (2019) 40(3):789–824. DOI: 10.1210/er.2018-00163
- Roos A, Bakker SJL, Links TP, Gans RO B and Wolffenbuttel BHR. Thyroid function is associated with components of the metabolic syndrome in euthyroid subjects. *The Journal of Clinical Endocrinology and Metabolism* (2007) 92(2): 491–496. <https://doi.org/10.1210/jc.2006-1718>.
- Prieto-Almeida F, Panveloski-Costa AC, Crunfli F, Da Silva Teixeira S, Nunes MT, Torrao AS. Thyroid hormone improves insulin signaling and reduces the activation of neurodegenerative pathway in the hippocampus of diabetic adult male rats. *Life Sci.* (2018) 192: 253–258. DOI: 10.1016/j.lfs.2017.11.013
- Vazquez-Anaya G, Martinez B, Soñanez-Organis JG, Nakano D, Nishiyama A, Ortiz RM. Exogenous thyroxine improves glucose intolerance in insulin resistant rats. *J Endocrinol.* (2017) 232:501–11. doi: 10.1530/JOE-16-0428. doi: 10.1530/JOE-16-0428
- Pickering D, Marsden J. How to measure blood glucose? *Community Eye Health.* 2014;27(87):56-7. PMID: 25918470; PMCID: PMC4322747
- Bancroft JD and Layton C. The hematoxylin and eosin, connective, and mesenchymal tissues with their stains. In: Suvarna SK, Layton C and Bancroft JD, editors. *Bancroft's theory and practice of histological techniques*. 7th edition. Churchill Livingstone: Philadelphia (2013) 173- 212. p
- Hany K. Mostafa: Effect of Diabetes Mellitus on the Structure of Skeletal Muscle in Adult Male Albino Rats and the Protective Role of Chromium: Histological and Immunohistochemical Study. *Egypt. J. Histol.* Vol. 31, No.2, Dec. 2008:341.
- Sawilowsky SS. Statistical pronouncements IV. *Journal of Modern Applied Statistical Methods* (2005) 4(2): 627-628. DOI: 10.22237/jmasm/1130804940
- Augusto V, Padovani C, Eduardo G and Campos R. Skeletal muscle fiber types in C57BL6J mice. *J. Morphol. Sci* (2004) 21: 89–94.
- Murgia M, Toniolo L, Nagaraj N, Ciciliot S, Vindigni V, Schiaffino S, Reggiani C, and Mann M. Single Muscle Fiber Proteomics Reveals Fiber-Type-Specific Features of Human Muscle Aging. *Cell Reports* (2017) 19(11): 2396–2409. DOI: 10.1016/j.celrep.2017.05.054

17. Lee SM, Lee M, C, Bae W, R, Yoon K, J, and Moon HY. Muscle fiber type-dependence effect of exercise on genomic networks in aged mice models. *Aging* (2022) 14(8): 3337–3364. DOI: 10.18632/aging.204024
  18. Faitg, J., Leduc-Gaudet, J.-P., Reynaud, O., Ferland, G., Gaudreau, P., and Gousspillou, G. (2019). Effects of Aging and Caloric Restriction on Fiber Type Composition, Mitochondrial Morphology and Dynamics in Rat Oxidative and Glycolytic Muscles. *Frontiers in Physiology* (2019) 10-15. DOI: 10.3389/fphys.2019.00420
  19. Rice, K. M., and Blough, E. R. Sarcopenia-related apoptosis is regulated differently in fast- and slow-twitch muscles of the aging F344/N×BN rat model. *Mechanisms of Ageing and Development* (2006) 127(8): 670–679. DOI: 10.1016/j.mad.2006.03.005
  20. Rice KM, Manne ND, Gadde MK, Paturi S, Arvapalli R, and Blough E. Differential regulation of apoptosis in slow and fast twitch muscles of aged female F344BN rats. *AGE* (2015) 37(2): 30-35. DOI: 10.1007/s11357-015-9767-z
  21. Tezze C, Romanello V, Desbats MA, Fadini GP, Albiero M, Favaro G, Ciciliot S, Soriano ME, Morbidoni V, Cerqua C, Loeffler S, Kern H, Franceschi C, Salvioli S, Conte M, Blaauw B, Zampieri S, Salviati L, Scorrano L, and Sandri M. Age-Associated Loss of OPA1 in Muscle Impacts Muscle Mass, Metabolic Homeostasis, Systemic Inflammation, and Epithelial Senescence. *Cell Metabolism* (2017) 25(6): 1374-1389.e6. DOI: 10.1016/j.cmet.2017.04.021
  22. Rodríguez-Nuevo A, Díaz-Ramos A, Noguera E, Díaz-Sáez F, Duran X, Muñoz J, P, Romero M, Plana N, Sebastián D, Tezze C, Romanello V, Ribas F, Seco J, Planet E, Doctrow S, R, González J, Borràs M, Liesa M, Palacín M and Zorzano A. Mitochondrial DNA and TLR9 drive muscle inflammation upon Opa1 deficiency. *The EMBO Journal* (2018) 37(10): e96553. DOI: 10.15252/embj.201796553
  23. Touvier T, De Palma C, Rigamonti E, Scagliola A, Incerti E, Mazelin L, Thomas JL, D'Antonio M, Politi L, Schaeffer L, Clementi E and Brunelli S. Muscle-specific Drp1 overexpression impairs skeletal muscle growth via translational attenuation. *Cell Death and Disease* (2015) 6(2): e1663.; <https://doi.org/10.1038/cddis.2014.595>
  24. Favaro G, Romanello V, Varanita T, Andrea Desbats M, Morbidoni V, Tezze C, Albiero M, Canato M, Gherardi G, De Stefani D, Mammucari C, Blaauw B, Boncompagni S, Protasi F, Reggiani C, Scorrano L, Salviati L and Sandri M. DRP1-mediated mitochondrial shape controls calcium homeostasis and muscle mass. *Nature Communications* (2019) 10(1): 2576. <https://doi.org/10.1038/s41467-019-10226-9>
  25. Xu X, Wang B, Ren C, Hu J, Greenberg DA, Chen T, Xie L, Jin K. Age-related Impairment of Vascular Structure and Functions. *Aging Dis.* (2017) 8(5):590-610. doi: 10.14336/AD.2017.0430
  26. Muller-Delp J, Spier SA, Ramsey MW, Lesniewski LA, Papadopoulos A and Humphrey JD. Effects of aging on vasoconstrictor and mechanical properties of rat skeletal muscle arterioles. *Am J Physiol Heart Circ Physiol* (2002) 282: H1843-H1854. DOI: 10.1152/ajpheart.00666.2001
  27. Kujoth GC, Hiona A, Pugh TD, Someya S, Panzer K, Wohlgenuth SE, Hofer T, Seo AY, Sullivan R, Jobling WA, Morrow JD, Van Remmen H, Sedivy J, M, Yamasoba T, Tanokura M, Weindruch R, Leeuwenburgh C and Prolla TA. Mitochondrial DNA mutations, oxidative stress, and apoptosis in mammalian aging. *Science (New York, N.Y.)* (2005) 309(5733): 481–484. <https://doi.org/10.1126/science.1112125>
  28. Sebastián D, Soriano E, Segalés J, Irazoki A, Ruiz-Bonilla V, Sala D, Planet E, Berenguer Llergo A, Muñoz JP, Sanchez-Feutrie M, Plana N, Hernández-Alvarez M, Serrano A, Palacín M and Zorzano A. Mfn2 deficiency links age-related sarcopenia and impaired autophagy to activation of an adaptive mitophagy pathway. *The EMBO Journal* (2016) 35-39. <https://doi.org/10.15252/embj.201593084>
  29. Leduc-Gaudet J-P, Picard M, St-Jean Pelletier F, Sgarioni N, Auger M-J, Vallée J, Robitaille R, St-Pierre D, H, and Gousspillou G. Mitochondrial morphology is altered in atrophied skeletal muscle of aged mice. *Oncotarget* (2015) 6(20): 17923–17937. <https://doi.org/10.18632/oncotarget.4235>
  30. Picca A, Calvani R, Lorenzi M, Menghi A, Galli M, Vitiello R, Randisi F, Bernabei R, Landi F and Marzetti E. Mitochondrial dynamics signaling is shifted toward fusion in muscles of very old hip-fractured patients: Results from the Sarcopenia in Hip Fracture (SHIFT) exploratory study. *Experimental Gerontology* (2017) 96,63–67. <https://doi.org/10.1016/j.exger.2017.06.005>
  31. Iossa S, Mollica MP, Lionetti L, Crescenzo R, Botta M, Barletta A and Liverini G. Acetyl-L-carnitine supplementation differently influences nutrient partitioning, serum leptin concentration and skeletal muscle mitochondrial respiration in young and old rats. *The Journal of Nutrition* (2002) 132(4): 636–642. DOI: 10.1093/jn/132.4.636
  32. Stannard SR. and Johnson NA. Insulin resistance and elevated triglyceride in muscle: more important for survival than “thrifty” genes? *The Journal of Physiology* (2004) 554(Pt 3): 595–607. DOI: 10.1113/jphysiol.2003.053926
-

33. Zierath JR, Krook A and Wallberg-Henriksson H. Insulin action and insulin resistance in human skeletal muscle. *Diabetologia* (2000) 43(7): 821–835. DOI: 10.1007/s001250051457
34. Di Meo S, Iossa S and Venditti P. Skeletal muscle insulin resistance: role of mitochondria and other ROS sources. *The Journal of Endocrinology* (2017) 233(1): R15–R42. DOI: 10.1530/JOE-16-0598
35. Quiles J, Martínez E, Ibáñez S, Ochoa J, Martín Y, López-Frías M, Huertas J, and Mataix J. Ageing-Related Tissue-Specific Alterations in Mitochondrial Composition and Function Are Modulated by Dietary Fat Type in the Rat. *Journal of Bioenergetics and Biomembranes* (2003) 34: 517–524. DOI: 10.1023/a:1022530512096
36. Petersen KF, Befroy D, Dufour S, Dziura J, Ariyan C, Rothman DL, DiPietro L, Cline GW and Shulman GI. Mitochondrial dysfunction in the elderly: possible role in insulin resistance. *Science (New York, N.Y.)* (2003) 300(5622): 1140–1142. DOI: 10.1126/science.1082889
37. Bruce CR, Anderson MJ, Carey AL, Newman DG, Bonen A, Kriketos AD, Cooney GJ and Hawley JA. Muscle oxidative capacity is a better predictor of insulin sensitivity than lipid status. *The Journal of Clinical Endocrinology and Metabolism* (2003) 88(11): 5444–5451. DOI: 10.1210/jc.2003-030791
38. Wallace DC. A Mitochondrial Paradigm of Metabolic and Degenerative Diseases, Aging, and Cancer: A Dawn for Evolutionary Medicine. *Annual Review of Genetics* (2005) 39(1): 359–407. DOI: 10.1146/annurev.genet.39.110304.095751
39. Bornstein R, Gonzalez B. and Johnson S. C. Mitochondrial pathways in human health and aging. *Mitochondrion* (2020) 54: 72–84. <https://doi.org/10.1016/j.mito.2020.07.007>
40. Distefano G and Goodpaster BH. Effects of Exercise and Aging on Skeletal Muscle. *Cold Spring Harbor Perspectives in Medicine* (2018) 8(3): 333–337. doi: 10.1101/cshperspect.a029785
41. Zimmermann A, Madreiter-Sokolowski C, Stryeck S. and Abdellatif M. Targeting the Mitochondria-Proteostasis Axis to Delay Aging . In *Frontiers in Cell and Developmental Biology* (2021) 9: 656201. DOI: 10.3389/fcell.2021.656201
42. He S, Yan L, Zhu R, Wei H, Wang J, Zheng L, Zhang Y. Skeletal-Muscle-Specific Overexpression of Chrono Leads to Disruption of Glucose Metabolism and Exercise Capacity. *Life (Basel)* (2022) 12(8):1233–1237. <https://doi.org/10.3390/life12081233>
43. Czech MP. Insulin action and resistance in obesity and type 2 diabetes. *Nature Medicine* (2017) 23(7): 804–814. DOI: 10.1038/nm.4350
44. Kane LA, Lazarou M, Fogel AI, Li Y, Yamano K, Sarraf SA, Banerjee S, and Youle RJ. PINK1 phosphorylates ubiquitin to activate Parkin E3 ubiquitin ligase activity. *Journal of Cell Biology* (2014) 205(2): 143–153. <https://doi.org/10.1083/jcb.201402104>
45. Garcia S, Nissanka N, Mareco EA, Rossi S, Peralta S, Diaz F, Rotundo RL, Carvalho RF and Moraes CT. Overexpression of PGC-1 $\alpha$  in aging muscle enhances a subset of young-like molecular patterns. *Aging Cell* (2018) 17(2): e12707. DOI: 10.1111/acel.12707
46. Goljanek-Whysall K, Soriano-Arroquia A, McCormick R, Chinda C and McDonagh B. miR-181a regulates p62/SQSTM1, parkin, and protein DJ-1 promoting mitochondrial dynamics in skeletal muscle aging. *Aging Cell* (2020) 19(4):e13140. DOI: 10.1111/acel.13140
47. Yang S, Loro E, Wada S, Kim B, Tseng W,-J, Li K, Khurana T, S, and Arany Z. Functional effects of muscle PGC-1 $\alpha$  in aged animals. *Skeletal Muscle* (2020) 10(1): 14. <https://doi.org/10.1186/s13395-020-00231-8>
48. No MH, Heo JW, Yoo SZ, Kim CJ, Park DH, Kang JH, Seo DY, Han J and Kwak HB. Effects of aging and exercise training on mitochondrial function and apoptosis in the rat heart. *Pflügers Archiv - European Journal of Physiology* (2020) 472(2): 179–193. <https://doi.org/10.12965/jer.130002>
49. Woldt E, Sebti Y, Solt LA, Duhem C, Lancel S, Eeckhoutte J, Hesselink M, KC. Paquet C, Delhaye S, Shin Y, Kamenecka TM, Schaart G, Lefebvre P, Nevière R, Burris TP, Schrauwen P, Staels B, and Duez H. Rev-erb- $\alpha$  modulates skeletal muscle oxidative capacity by regulating mitochondrial biogenesis and autophagy. *Nature Medicine* (2013) 19(8): 1039–1046. <https://doi.org/10.1038/nm.3213>
50. Mayeuf-Louchart A, Thorel Q, Delhaye S, Beauchamp J, Duhem C, Danckaert A, Lancel S, Pourcet B, Woldt E, Boulinguez A, Ferri L, Zecchin M, Staels B, Sebti Y, and Duez H. Rev-erb- $\alpha$  regulates atrophy-related genes to control skeletal muscle mass. *Scientific Reports* (2017) 7(1): 14383. <https://doi.org/10.1371/journal.pone.0227720>
51. Gouspillou G, Sgarioto N, Kapchinsky S, Purves-Smith F, Norris B, Pion C, H, Barbat-Artigas S, Lemieux F, Taivassalo T, Morais JA, Aubertin-Leheudre M, and Hepple RT. Increased sensitivity to mitochondrial permeability transition and myonuclear translocation of endonuclease G in atrophied muscle of physically active older humans. *FASEB Journal : Official Publication of the Federation of American Societies for Experimental Biology* (2014) 28(4): 1621–1633. doi: 10.1096/fj.13-242750.

52. Wang W, Fang H, Groom L, Cheng A, Zhang W, Liu J, Wang X, Li K, Han P, Zheng M, Yin J, Wang W, Mattson M, P, Kao JP, Lakatta EG, Sheu SS, Ouyang K, Chen J, Dirksen RT and Cheng H. Superoxide flashes in single mitochondria. *Cell* (2008) 134(2): 279–290. <https://doi.org/10.1016/j.cell.2008.06.017>
53. Dodd SL, Gagnon BJ, Senf SM, Hain BA and Judge AR. Ros-mediated activation of NF-kappaB and Foxo during muscle disuse. *Muscle and Nerve* (2010) 41(1): 110–113. <https://doi.org/10.1002/mus.21526>
54. Liu Y, Bi, X, Zhang Y, Wang Y and Ding W. Mitochondrial dysfunction/ NLRP3 inflammasome axis contributes to angiotensin II-induced skeletal muscle wasting via PPAR- $\gamma$ . *Laboratory Investigation* (2020) 100(5): 712–726. <https://doi.org/10.1038/s41374-019-0355-1>
55. Wang XH, Zhang L, Mitch WE, LeDoux JM, Hu J and Du J. Caspase-3 cleaves specific 19 S proteasome subunits in skeletal muscle stimulating proteasome activity. *The Journal of Biological Chemistry* (2010) 285(28): 21249–21257. <https://doi.org/10.1074/jbc.M109.041707>
56. Mullur R, Liu YY and Brent GA. Thyroid Hormone Regulation of Metabolism. In *Physiological Reviews* (2014) 94(2): 355–382. <https://doi.org/10.1152/physrev.00030.2013>
57. Bianco AC, Dumitrescu A, Gereben B, Ribeiro MO, Fonseca T., Fernandes GW and Bocco BM. Paradigms of Dynamic Control of Thyroid Hormone Signaling. *Endocrine Reviews* (2019) 40(4): 1000–1047. <https://doi.org/10.1210/er.2018-00275>
58. Wulf A, Harneit A, Kröger M, Kebenko M, Wetzel MG and Weitzel JM. T3-mediated expression of PGC-1alpha via a far upstream located thyroid hormone response element. *Molecular and Cellular Endocrinology* (2008) 287(1–2): 90–95. <https://doi.org/10.1016/j.mce.2008.01.017>
59. Liang H and Ward WF. PGC-1alpha: a key regulator of energy metabolism. *Advances in Physiology Education* (2006) 30(4): 145–151. <https://doi.org/10.1152/advan.00052.2006>
60. Crescenzo R Bianco F, Mazzoli A, Giacco A, Liverini G and Iossa S. Mitochondrial efficiency and insulin resistance. *Frontiers in Physiology* (2014) 5: 512. doi: 10.3389/fphys.2014.00512
61. Milanese A, Lee JW, Yang A, Liu YY, Sedrakyan S, Cheng SY, Perin L and Brent GA. Thyroid Hormone Receptor Alpha is Essential to Maintain the Satellite Cell Niche During Skeletal Muscle Injury and Sarcopenia of Aging. *Thyroid: Official Journal of the American Thyroid Association* (2017) 27(10): 1316–1322. <https://doi.org/10.1089/thy.2017.0021>
62. Saltiel AR and Kahn CR. Insulin signalling and the regulation of glucose and lipid metabolism. *Nature* (2001) 414(6865): 799–806. <https://doi.org/10.1038/414799a>
63. van Loon LJ and Goodpaster BH. Increased intramuscular lipid storage in the insulin-resistant and endurance-trained state. *Pflugers Archiv: European Journal of Physiology* (2006) 451(5): 606–616. <https://doi.org/10.1007/s00424-005-1509-0>
64. Izumiya Y, Hopkins T, Morris C, Sato K, Zeng L, Viereck J, Hamilton JA, Ouchi N, LeBrasseur NK and Walsh K. Fast/Glycolytic muscle fiber growth reduces fat mass and improves metabolic parameters in obese mice. *Cell Metabolism* (2008) 7(2): 159–172. <https://doi.org/10.1016/j.cmet.2007.11.003>
65. Strączkowski M, Nikolajuk A, Stefanowicz M, Matulewicz N, Fernandez-Real JM and Karczewska-Kupczewska M. Adipose Tissue and Skeletal Muscle Expression of Genes Associated with Thyroid Hormone Action in Obesity and Insulin Resistance. *Thyroid: Official Journal of the American Thyroid Association* (2022) 32(2): 206–214. <https://doi.org/10.1089/thy.2021.0351>
66. Simonides WS, Thelen MH, van der Linden CG, Muller A and van Hardeveld C. Mechanism of thyroid-hormone regulated expression of the SERCA genes in skeletal muscle: implications for thermogenesis. *Bioscience Reports* (2001) 21(2): 139–154. <https://doi.org/10.1023/a:1013692023449>

## الملخص العربي

## دراسة نسيجية ومورفومترية حول تأثير ثلاثي يودوثيرونين على التغيرات النسيجية في عضلة ساق ذكر الجرذ الأبيض المسن المصاحبة لضعف الغدة الدرقية

أسماء إبراهيم احمد<sup>1</sup>، سحر محمد توفيق العجاتي<sup>2</sup>، سيد مصطفى السيد<sup>1</sup>

<sup>1</sup> قسم التشريح وعلم الأجنة، <sup>2</sup> قسم الفسيولوجيا، كلية الطب، جامعة عين شمس، القاهرة، مصر

**المقدمة:** الشيخوخة المرتبطة بقصور الغدة الدرقية قد يصاحبها العديد من التغيرات الدقيقة في ألياف العضلات الهيكلية، والتي يكون سببها انخفاض ثلاثي يودوثيرونين، ارتفاع السكر في الدم وزيادة أنسولين الدم. ثلاثي يودوثيرونين يمكنه ان ينشط عملية التمثيل الغذائي للجلوكوز ويقلل من ارتفاع السكر في الدم ويقلل من عدم الاستجابة للأنسولين في الألياف العضلية الهيكلية في الحالات التي يكون فيها مستوى ثلاثي يودوثيرونين منخفضاً في الدم.

**الهدف من العمل:** تقييم التغيرات النسيجية لعضلة ساق الجرذ الابيض في عمر الشيخوخة المرتبطة بقصور الغدة الدرقية وكذلك الاختلافات الكيميائية الحيوية والدور الوقائي المحتمل لثلاثي يودوثيرونين.

**المواد والطرق:** تم استخدام ثلاثين ذكر من الجرذان البيضاء. قسمت الجرذان إلى ثلاث مجموعات، بواقع عشرة جرذان في كل مجموعة. المجموعة الأولى الجرذان البالغين، المجموعة الثانية الجرذان في عمر الشيخوخة، المجموعة الثالثة من الجرذان في عمر الشيخوخة المعالجة بثلاثي يودوثيرونين.

تم إعطاء ثلاثي يودوثيرونين بجرعة ٨ ميكروغرام / كجم من وزن الجسم لمدة أسبوعين. في نهاية التجربة، تم تشريح عضلات الساق وتحضير شرائح لتصبغ بصبغة الهيماتوكسيلين والإيوسين، وصبغة ماسون ثلاثية الألوان، وشرائح أخرى شبيهة رقيقة لصبغها بالتولويدين الأزرق، وشرائح أخرى لدرستها بالمجهر الإلكتروني ثم اجريت القياسات المورفولوجية.

**النتائج:** أظهرت العضلات الهيكلية للمجموعة الثانية من الجرذان في عمر الشيخوخة ترقق في بعض الألياف العضلية، وفقدان التخطيطات اوالتحزرات العرضية وضمور في نواة اللييفات العضلية. تم الكشف عن التهابات في صورة ارتشاح خلوي أحادي النواة بين الالياف العضلية الهيكلية مع ترسبات الخلايا الدهنية. أظهرت المقاطع الرقيقة جدا اضطراباً ملحوظاً في اللييفات العضلية مع العديد من الميتوكوندريا المتحللة الكبيرة ذات الشكل غير الطبيعي. أظهرت المجموعة الثالثة استعادة البنية الطبيعية لألياف العضلات الهيكلية.

وجد انخفاض في سمك ألياف العضلات وزيادة ترسب ألياف الكولاجين في المجموعة الثانية في الجرذان في عمر الشيخوخة ذو دلالة إحصائية كبيرة وحدث تحسن لهذه التغييرات في المجموعة الثالثة بفضل ثلاثي يودوثيرونين مع زيادة ذات دلالة احصائية في نسبة الجلوكوز و الانسولين في الدم في المجموعة الثانية وتم التحكم فيها في المجموعة الثالثة.

**الخلاصة:** الشيخوخة المرتبطة بضعف الغدة الدرقية احدثت تغييرات نسيجية ملحوظة في العضلات الهيكلية لذكر الجرذ الابيض و امكن التحكم فيها باعطاء ثلاثي يودوثيرونين من خلال قدرته علي زيادة الاستجابة للأنسولين. ويمكن من الناحية الاكلينيكية القيام بعمل المزيد من الدراسات علي استخدام ثلاثي يودوثيرونين في المسنين الذين يعانون من ضعف العضلات المصاحب لقصور الغدة الدرقية.